Biophysical Chemistry 136 (2008) 145–151

Contents lists available at ScienceDirect

Biophysical Chemistry

journal homepage: http://www.elsevier.com/locate/biophyschem

Protein effective rotational correlation times from translational self-diffusion coefficients measured by PFG-NMR

Shenggen Yao *[,1], Jeffrey J. Babon [1], Raymond S. Norton

The Walter and Eliza Hall Institute of Medical Research, 1G Royal Parade, Parkville, VIC 3050, Victoria, Australia

ARTICLE INFO

Article history:
Received 26 February 2008
Received in revised form 4 June 2008
Accepted 6 June 2008
Available online 14 June 2008

Keywords:
Collective ^{15}N relaxation parameters
Hydrodynamic calculations
Effective rotational correlation time
PFG-NMR
Translational diffusion coefficient

ABSTRACT

Molecular rotational correlation times are of interest for many studies carried out in solution, including characterization of biomolecular structure and interactions. Here we have evaluated the estimates of protein effective rotational correlation times from their translational self-diffusion coefficients measured by pulsed-field gradient NMR against correlation times determined from both collective and residue-specific ^{15}N relaxation analyses and those derived from 3D structure-based hydrodynamic calculations. The results show that, provided the protein diffusive behavior is coherent with the Debye–Stokes–Einstein model, translational diffusion coefficients provide rapid estimates with reasonable accuracy of their effective rotational correlation times. Effective rotational correlation times estimated from translational diffusion coefficients may be particularly beneficial in cases where i) isotopically labelled material is not available, ii) collective backbone ^{15}N relaxation rates are difficult to interpret because of the presence of flexible termini or loops, or iii) a full relaxation analysis is practically difficult because of limited sensitivity owing to low protein concentration, high molecular mass or low temperatures.

1. Introduction

Knowledge of the effective rotational correlation times is of significant value in biophysical characterization of biomolecules in solution. The rotational correlation time of a protein in solution can be rigorously determined from its experimentally measured backbone relaxation parameters if its 3D structure is known [1]. An effective rotational correlation time, τ_c, defined by an isotropic rigid rotor, is often estimated from the ratios of backbone transverse and longitudinal ^{15}N relaxation rates, R_2/R_1, of residues not experiencing slow timescale/large amplitude internal motion or chemical/conformational exchange [2–4]. In order to identify those residues with significant internal motion (i.e. residues experiencing slow timescale/large amplitude internal motion or involved in chemical/conformational exchange), and for them to be excluded from the determination of τ_c, residue-specific ^{15}N R_1 and R_2 values need to be obtained. Alternatively, collective ^{15}N relaxation rates of backbone amides have been used for rapid estimates of protein effective rotational correlation times [5,6]. This kind of rapid estimation of τ_c is beneficial, in particular when a full relaxation analysis is practically hindered due to limited sensitivity, for example in cases of inadequate protein concentration, high molecular mass or low temperatures. However, the inevitable inclusion of residues with significant internal motion in the estimation of rotational correlation time from collective ^{15}N relaxation rates makes the resulting τ_c a lower limit of the actual value, with the extent of underestimation depending on the details of internal motion of the protein [6]. Collective ^{15}N relaxations rates may therefore result in a severe underestimation of the rotational correlation time if substantial local motion is present.

Protein translational self-diffusion coefficients, which are readily measurable by pulsed-field-gradient NMR (PFG-NMR), have been used widely to characterize protein/peptide self-association and aggregation [7,8], amide exchange [9], folding and unfolding [10] and ligand binding [11]. Given that molecular translational and rotational diffusion are well described by the Stokes–Einstein and the Debye–Stokes–Einstein equations, experimentally measured self-diffusion coefficients have been employed previously to calculate protein hydrodynamic radius, R_h [12], as well as for the estimation of protein rotational correlation times [13,14]. Here we have further explored the suitability of translational self-diffusion coefficients measured by PFG-NMR for rapid estimation of protein effective rotational times using a protein complex in the presence of a reference molecule. The resultant effective rotational correlation times calculated directly from translational diffusion coefficients are compared with those determined from collective and residue-specific ^{15}N relaxation analyses, as well as those obtained from 3D structure-based hydrodynamic calculations. Our results show that a rapid estimate of rotational correlation time of a protein/protein complex, which is otherwise difficult to determine by

Abbreviations: ElonBC-SB, mouse elongins B and C and the SOCS box domain of SOCS-3 complex.

* Corresponding author. Tel.: +61 3 93452332; fax: +61 3 93470852.
E-mail address: syao@wehi.edu.au (S. Yao).

[1] These authors contributed equally to this work.

0301-4622/$ – see front matter © 2008 Elsevier B.V. All rights reserved.
doi:10.1016/j.bpc.2008.06.002

alternative means, can be obtained exclusively from translational diffusion coefficients measured by PFG-NMR (Eq. (6)) with reasonable accuracy.

2. Experimental

Measurements were carried out primarily on a ^{15}N-labelled 30 kDa ternary protein complex of mouse elonginB, elonginC and the SOCS box domain of SOCS3 (termed ElonBC-SB) using a Bruker DRX600 spectrometer with a 5 mm triple resonance probe (equipped with triple gradients). A detailed description of expression and purification of this ternary complex as well as a table summarizing NMR experiments performed (Table S1) are given in the Supplementary data. Dioxane, with a published hydrodynamic radius of 2.12 Å [12], was used as a an internal reference molecule. For the evaluation of small molecules other than dioxane as alternative internal references, a second sample containing dioxane, DMSO, acetone, and acetonitrile was prepared in a similar buffer solution to that used for ElonBC-SB.

Pulsed field gradient strengths were calibrated initially by measuring the self-diffusion coefficient of residual H_2O in a freshly prepared 100% ^2H_2O sample (99.96 ^2H_2O from CIL, catalog No: DLM-6) at 298 K. A diffusion coefficient of 1.9×10^{-9} m^2 s^{-1} for the residual H_2O signal [15] was used for back calculation of the field gradient strengths. The pulsed field gradient strengths (G_x and G_y) were further calibrated against the dimension of a standard 5 mm NMR sample tube (an internal diameter of 4.24 mm, Wilmad-Labglass, part No 535-pp-7) using a 1D gradient echo sequence. The two methods resulted in almost identical calibration values (within 1%) for both G_x and G_y.

Translational self-diffusion coefficients were measured using a longitudinal eddy-current delay stimulated echo (LEDSTE) sequence [16] incorporating a WATERGATE segment for water suppression [17], as described previously [8]. For each measurement, a series of 12 diffusion weighted 1D spectra was recorded in a 2D manner using gradient pulses of 6 ms duration, a separation of 50.8 ms, and field gradient strengths ranging from 2.5 to 31 G cm^{-1} applied in either the x or y direction (G_x and G_y). All measurements were repeated with shorter gradient pulse durations of 2 ms and a corresponding separation of 46.8 ms in order to facilitate measurements of the more rapid diffusion rate of dioxane compared to ElonBC-SB. Translational diffusion coefficients, D_t, were obtained by fitting peak intensities to the following equation using the T_1/T_2 *relaxation* routine in TOPSPIN (Version 1.3 Bruker BioSpin):

$$I = I_0\exp\left\{-\gamma^2 g^2\delta^2(\Delta-\delta/3)D_t\right\} \tag{1a}$$

where γ is the ^{1}H gyromagnetic ratio and g, δ and Δ are the amplitude, duration and separation of the gradient pulses, respectively. For ElonBC-SB, translational diffusion coefficients averaged over a number of peaks in the aliphatic regions as well as over values measured with the diffusion encoding field gradient applied in either the x or y direction are reported. Similarly, for dioxane, reported values are also those averaged over values measured with G_x and G_y.

A two-component fit was also considered for dioxane in order to take into account possible contributions from resonances from ElonBC-SB that may have overlapped with the resonance of dioxane using the following equation:

$$I = I_0^{\mathrm{REF}}\exp\left\{-\gamma^2 g^2\delta^2(\Delta-\delta/3)D_t^{\mathrm{REF}}\right\} + I_0\exp\left\{-\gamma^2 g^2\delta^2(\Delta-\delta/3)D_t\right\} \tag{1b}$$

where D_t^{REF} and D_t represent translational diffusion coefficients of the reference molecule, dioxane, and ElonBC-SB with D_t being fixed at the diffusion coefficient of the complex as obtained from Eq. (1a). No significant improvement was found for translational diffusion coefficients of dioxane obtained with Eq. (1b) in comparison with Eq. (1a) as the signal of dioxane is much stronger than that of background protein in the present study. Therefore, only the fitting results from Eq. (1a) are reported.

The dependence of the translational and rotational diffusion coefficients on solution viscosity (η) and hydrodynamic radius (R_h) is described by the Stokes-Einstein equation and the Debye–Stokes–Einstein equation, respectively:

$$D_t = k_B T/(6\pi\eta R_h) \tag{2}$$

$$D_r = k_B T/(8\pi\eta R_h^3) \tag{3}$$

where k_B is the Boltzmann constant and T is the absolute temperature. The rotational correlation time, τ_c, can thus be expressed as a function of η and R_h:

$$\tau_c = 1/(6D_r) = (4/3)\left[\pi\eta R_h^3/(k_B T)\right] \tag{4a}$$

or η and D_t:

$$\tau_c = 1/(6D_r) = (1/162)\left[k_B^2 T^2/(\pi^2\eta^2 D_t^3)\right] \tag{4b}$$

or R_h and D_t:

$$\tau_c = 1/(6D_r) = (2/9)R_h^2/D_t \tag{4c}$$

In the presence of a reference molecule with known hydrodynamic radius, the hydrodynamic radius of a protein, R_h, can be obtained from its translational diffusion coefficient, D_t, using the following equation [18]:

$$R_h = R_h^{\mathrm{REF}}\left(D_t^{\mathrm{REF}}/D_t\right) \tag{5}$$

where R_h^{REF} and D_t^{REF} are the hydrodynamic radius and translational diffusion coefficient of the reference molecule, respectively. Eq. (4c) can be rearranged as:

$$\tau_c = (2/9)\left(R_h^{\mathrm{REF}} D_t^{\mathrm{REF}}\right)^2/(D_t)^3 \tag{6}$$

Clearly, from Eq. (6), the effective rotational correlation times can be calculated exclusively from experimentally measured translational diffusion coefficients of a protein or protein complex, D_t, and translational diffusion coefficient of a reference molecule, D_t^{REF}, with a known hydrodynamic radius, R_h^{REF}. In the present study, dioxane was used as the reference molecule, with a hydrodynamic radius of 2.12 Å [12].

Collective ^{15}N relaxation rates, R_1 and R_2, of backbone amides were measured from the first-increment FIDs of ^{15}N relaxation weighted ^{15}N-HSQC spectra at temperatures of 283, 288, 293, 298, 303, 310 and 318 K using standard pulse sequences in the Bruker pulse sequence library similar to those published previously [19]. Collective R_1 and R_2 values were obtained by fitting the integrals of all peaks across the amide region (6.0–12.0 ppm) to a two-parameter exponential decay (Eq. (7a)) using the T_1/T_2 *relaxation* subroutine in TOPSPIN (Version 1.3 Bruker BioSpin). In contrast to the collective backbone ^{15}N R_1 decay curves, which fit satisfactorily to a single two-parameter exponential decay, ^{15}N R_2 decay curves clearly deviated from a single two-parameter exponential decay. A dual two-parameter exponential decay fit was subsequently performed (Eq. (7b)) for R_2 using SigmaPlot (version 8.0, Systat Software)

$$I(t) = I(0)\exp(-tR_i), \quad i = 1,2 \tag{7a}$$

$$I(t) = I_f(0)\exp(-tR_{2f}) + I_s(0)\exp(-tR_{2s}) \tag{7b}$$

where R_{2s} and R_{2f} represent the slower and faster components of collective ^{15}N R_2 rates, respectively. Effective rotational correlation times of ElonBC-SB were then estimated from its collective ^{15}N R_{2f}/R_1 ratios using the program *tmest* within the *Modelfree* software package (A.G. Palmer, Columbia University). Rotational correlation times of ElonBC-SB were also estimated from collective backbone ^{15}N relaxation

rates of α- and β-spin states measured at 283, 288, 293, 298, 310 and 318 K using the TRACT sequences described recently [6]. A total of 48 relaxation delays was used with a recycle time of 2.5 s and 256 scans per relaxation delay. R_α and R_β rates were subsequently obtained by fitting the integrals of all peaks across the amide region (6.0–12.0 ppm) to a two-parameter exponential decay (Eq. (7a)) and a dual two-parameter exponential decay (Eq. (7b)) for R_α and R_β using the T_1/T_2 relaxation subroutine in TOPSPIN (Version 1.3 Bruker BioSpin) and/or *SigmaPlot* (version 8.0, SYSTAT Software). The R_α and R_β rates were then used to calculate the effective correlation times as described by Lee et al. [6].

Hydrodynamic parameters of ElonBC-SB were calculated from both the closest-to-mean structure of a family of 20 structures of ElonBC-SB in solution (Babon et al., J. Mol. Biol., in press) and the crystal structure of the SOCS2-elonginBC complex (only including the SOCS box fragment (160–198), elongonBC+SOCS2$^{160-198}$, PDB accession code 2C9W [20] using the program HYDRONMR (version 5a) [21], with the viscosity of water [22] as an approximation of that for the protein solution.

3. Results and discussion

This three-protein complex, ElonBC-SB, was chosen as it is sufficiently stable to allow measurements over a range of temperatures and it represents a 'real life' situation where the presence of unstructured regions can dominate collective ^{15}N relaxation rates and make rapid τ_c estimation difficult in the absence of a residue-specific relaxation analysis. SOCS box proteins form stable ternary complexes with the elonginBC. As shown in Fig. 1, ElonBC-SB is well structured in solution and retains its predominant structural elements (Babon et al., J. Mol. Biol., in press) as seen in the crystal forms of SOCS2-elonginBC [20], even though local flexibility of several loop and terminal regions is clearly evident in the spectra of ElonBC-SB, as residues of these regions give resonances in narrowly dispersed and heavily crowded region (Supplementary data, Fig. S1). These flexible regions include the C-terminal half of the SOCS box peptide of SOCS-3, residues 99–115 of elongin B and residues 69–79 of elongin C (Babon et al., J. Mol. Biol., in press). Flexibility of several regions in the complex was also evident in the crystal structure of SOCS-2 and elonginBC complex [20]; for example, atomic coordinates were not defined for residues

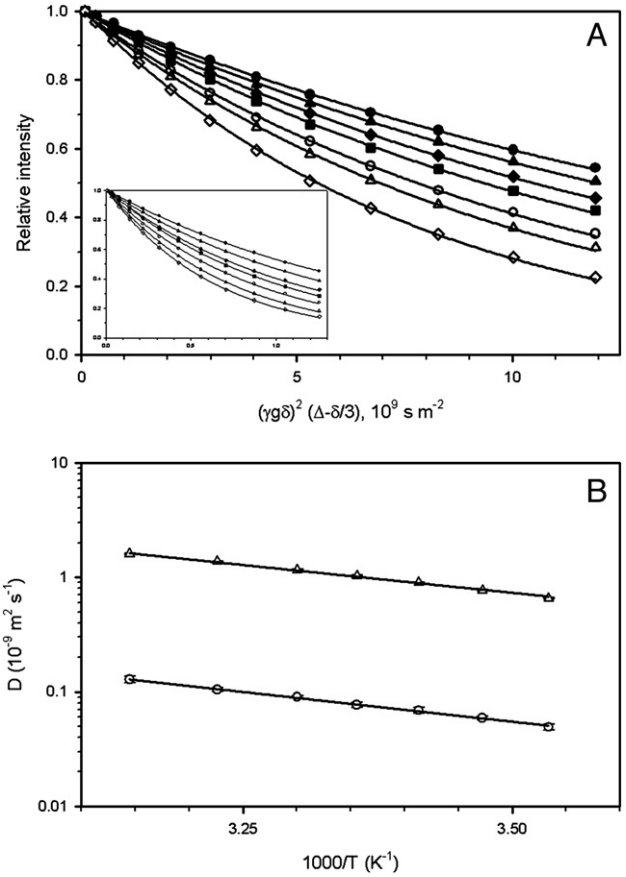

Fig. 2. Translational diffusion of ElonBC-SB and reference molecule dioxane. (A) Translational diffusion induced signal attenuation shown as relative intensities versus the strength of diffusion encoding, $\gamma^2g^2\delta^2(\Delta-\delta/3)$, (283 K (●), 288 K (▲), 293 K (♦), 298 K (■), 303 K (○), 310 K (Δ) and 318 K (◊)) for ElonBC-SB with corresponding data for dioxane shown in the inset. All the lines represent the results of nonlinear regression to Eq. (1a). (B) Experimentally measured translational diffusion coefficients of ElonBC-SB and dioxane versus 1000/T. The temperature dependence of translational diffusion coefficients of both ElonBC-SB and dioxane are very well described by an Arrhenius function (lines).

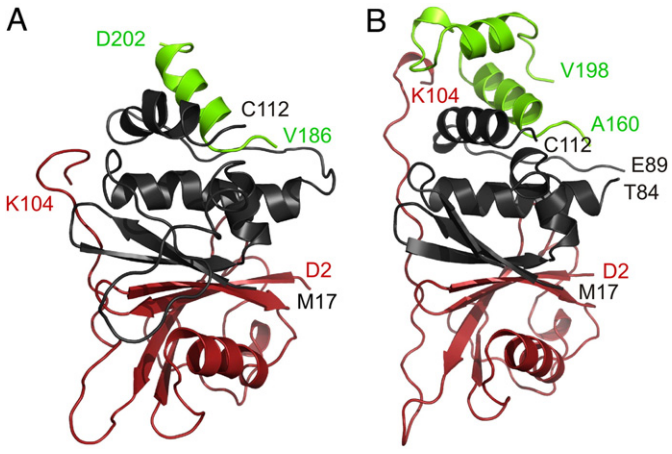

Fig. 1. Ribbon diagrams of solution structure of mouse elonginBC in complex with the SOCS box domain of SOCS3 (A, residues from D203 to L225 of the SOCS box domain of SOCS3 in solution were not defined) and crystal structure of elonginBC in complex with SOCS2 (B, only showing the SOCS box fragment of SOCS2, residues 160–198) [20]. Colour schemes: SOCS box fragment: green, elongin B: red, and elongin C: black. In the crystal structure of elonginBC in complex with SOCS2 (B) atomic coordinates are not defined for residues 105–118 of elongin B and residues 46–57 and 85–87 of elongin C.

105–118 of elongin B and residues 46–57 and 85–87 of elongin C as a consequence of missing electron density in the X-ray diffraction map.

Translational self-diffusion induced signal attenuation *versus* the strength of diffusion encoding, $\gamma^2g^2\delta^2(\Delta-\delta/3)$, and Arrhenius plots showing the temperature dependence of diffusion coefficients for both ElonBC-SB and dioxane are presented in Fig. 2. Diffusion coefficients of both ElonBC-SB and dioxane over this temperature range are described very well by the Arrhenius function, indicating that their diffusive behaviour is coherent with the Stokes–Einstein model. Experimental translational diffusion coefficients, calculated hydrodynamic radii (Eq. (5)), and effective rotational correlation times (Eq. (6)) of ElonBC-SB for temperatures ranging from 283 to 318 K are summarized in Table 1. Translational diffusion coefficients of ethylenediamine tetraacetic acid (EDTA), a common addition to the buffer solution for protein samples used for structural studies, and apparent hydrodynamic radius calculated from its translational diffusion coefficient using Eq. (5) are also given in Table 1. Under the present conditions, EDTA gave apparent hydrodynamic radii ranging from 4.35 to 4.54 Å with an averaged value of 4.46±0.07 Å.

Similar values were obtained from hydrodynamic calculations performed using the closest-to-mean structure of a family of 20 structures of ElonBC-SB in solution (Babon et al., J. Mol. Biol., in press) and the crystal structure of the SOCS2 SOCS box (SOCS-2$^{160-198}$) in complex with elonginBC, elongonBC+SOCS2$^{160-198}$, the closest

Table 1
Translational diffusion coefficients and effective rotational correlation times of ElonBC-SB

T (K)	D_t^{REF} [a] (10^{-9} m^2 s^{-1})	D_t [b] (10^{-11} m^2 s^{-1})	R_h [c] (Å)	τ_c [d] (ns)	D_t^{HYDRO} [e] (10^{-11} m^2 s^{-1})	τ_c^{HYDRO} [e] (ns)	D_t^{EDTA} [f] (10^{-9} m^2 s^{-1})	R_h^{EDTA} [f] (Å)
283	0.66±0.02	4.92±0.3	28.2	35.9 (31.5)	5.89 (5.45)	30.8 (37.7)	0.31±0.01	4.51
288	0.77±0.01	5.90±0.2	27.6	28.8 (25.4)	6.88 (6.37)	26.4 (32.3)	0.36±0.01	4.53
293	0.90±0.01	6.88±0.4	27.7	24.7 (22.0)	7.96 (7.36)	22.8 (27.9)	0.42±0.01	4.54
298	1.03±0.02	7.91±0.4	27.6	21.4 (19.0)	9.10 (8.43)	19.9 (24.4)	0.49±0.01	4.46
303	1.16±0.01	8.99±0.2	27.3	18.5 (16.3)	10.30 (9.57)	17.6 (21.5)	0.55±0.01	4.47
310	1.37±0.02	10.46±0.4	27.7	16.3 (14.41)	12.20 (11.29)	14.9 (18.2)	0.66±0.01	4.40
318	1.60±0.02	12.85±0.8	26.4	12.1 (10.5)	14.50 (13.40)	12.5 (15.3)	0.78±0.01	4.35

[a] Experimentally measured translational diffusion coefficients of reference molecule, dioxane, shown as average value±standard deviation.
[b] Experimentally measured translational diffusion coefficients of ElonBC-SB and standard deviation, shown as average value±standard deviation.
[c] Hydrodynamic radii of ElonBC-SB calculated from experimentally measured translational diffusion coefficients using Eq. (5).
[d] Effective rotational correlation times of ElonBC-SB calculated using Eq. (6). Corresponding values calculated from translational diffusion derived R_h value (column 4) using the viscosities of H_2O are shown in parentheses.
[e] Translational diffusion coefficients and rotational correlation times of ElonBC-SB calculated using HYDRONMR with an atomic element radius (AER) of 3.1 Å from crystal structure of elongonBC+SOCS2$^{160-198}$. Corresponding values for AER of 5.0 Å are shown in parentheses. Hydrodynamic radii calculated are 26.9 Å for an AER of 3.1 Å and 29.1 Å for an AER of 5.0 Å, respectively.
[f] Translational diffusion coefficients of ethylenediamine tetraacetic acid (EDTA) and apparent hydrodynamic radius calculated from its translational diffusion coefficient using Eq. (5). In the present study, EDTA gave apparent hydrodynamic radii ranging from 4.35 to 4.54 Å with an averaged value of 4.46±0.07 Å. It is worth noting that the apparent translational diffusion coefficient of EDTA may vary upon binding of ions.

homologue in the Protein Data Bank [20] and data from the latter were reported. Hydrodynamic radii calculated from the crystal structure of, elongonBC+SOCS2$^{160-198}$ with atomic element radii (AER) of 3.1 and 5.0 Å (representing the lower and upper limits of the typical range of AER [21]) are 26.9 and 29.1 Å, respectively. Corresponding translational diffusion coefficients and rotational correlation times of ElonBC-SB from hydrodynamic calculations of elongonBC+SOCS2$^{160-198}$ are summarized in Table 1. While hydrodynamic radii, R_h, derived from translational diffusion coefficients of ElonBC-SB agree very well with calculated values across the temperature range studied, experimentally measured translational diffusion coefficients were found to be systematically lower than those from hydrodynamic calculations (Table 1), as reported previously [23]. These lower experimentally measured translational diffusion coefficients resulted in apparently higher τ_c values for ElonBC-SB (Eq. (6) and Table 1).

It has been shown previously that a quick estimation of protein rotational correlation time can be obtained from its collective ^{15}N relaxation parameters without the need for a residue-specific relaxation analysis [5,6]. In order to compare rotational correlation times derived from translational diffusion coefficients with τ_c estimated from collective ^{15}N relaxation measurements, collective ^{15}N relaxation parameters of ElonBC-SB were also measured using both conventional pulse sequences as well as the recently reported TRACT sequences [6]. Decay curves of collective ^{15}N R_1 and R_2 and single-spin-state R_α and R_β rates of ElonBC-SB at several temperatures are shown in Figs. 3 and 4, respectively. In contrast to collective backbone ^{15}N R_1 decay curves, which fit satisfactorily to a single two-parameter exponential decay (Fig. 3A), ^{15}N R_2 decay curves clearly deviate from a single two-parameter exponential decay (Fig. 3B, dashed lines). This is consistent with the fact that internal motion has much more profound effects on R_2 than R_1. It was found subsequently that the collective backbone ^{15}N R_2 decay curves could be fitted satisfactorily to a dual two-parameter exponential decay (Fig. 3B, solid lines). The faster component, R_{2f}, was thus taken as an approximation of the collective R_2 value from residues less affected by internal motion and was chosen for the estimation of effective rotational correlation times of the ElonBC-SB complex. Similarly, for the single-spin-state relaxation rates, both R_α and R_β decay curves also deviate from a single two-parameter exponential fit, particularly at lower temperatures (Fig. 4). Again, a dual two-parameter exponential decay was found to give very good fits at lower temperatures. Experimentally measured collective ^{15}N relaxation rates and subsequently calculated rotational correlation times are summarized in Table 2. Residue-specific backbone ^{15}N R_1 and R_2 rates were obtained for ElonBC-SB at 310 and 318 K (Supplementary Material, Figs. S1 and S2 and Table S2). Overall averaged R_1, R_2 values for ElonBC-SB are 1.03±0.12 s^{-1} and 19.74±5.30 s^{-1} at 310 K and 1.52±0.20 s^{-1} and 13.55±3.30 s^{-1} at 318 K. Effective rotational correlation times of the complex calculated from averaged ratios of R_2/R_1 of backbone amides located in the structured regions are 14.5±0.7 and 9.6±0.5 ns for 310 and 318 K, respectively, as estimated using the

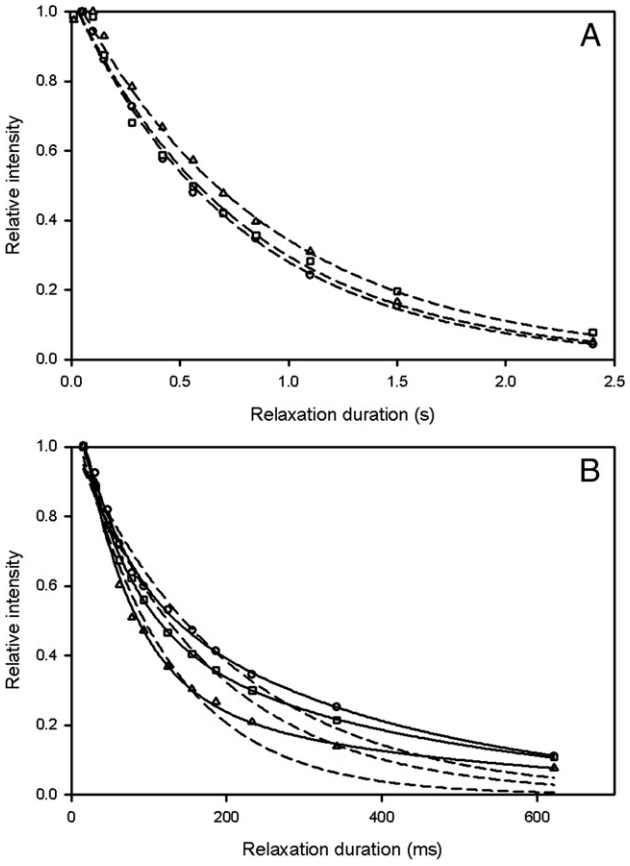

Fig. 3. Collective backbone ^{15}N relaxation decay curves of ElonBC-SB. (A) R_1 and (B) R_2 at 283 K (○), 293 K (□) and 310 K (Δ). Dashed lines represent the results of nonlinear regression of a two-parameter single exponential decay whereas solid lines represent the results of nonlinear regression of a dual two-parameter exponential decay.

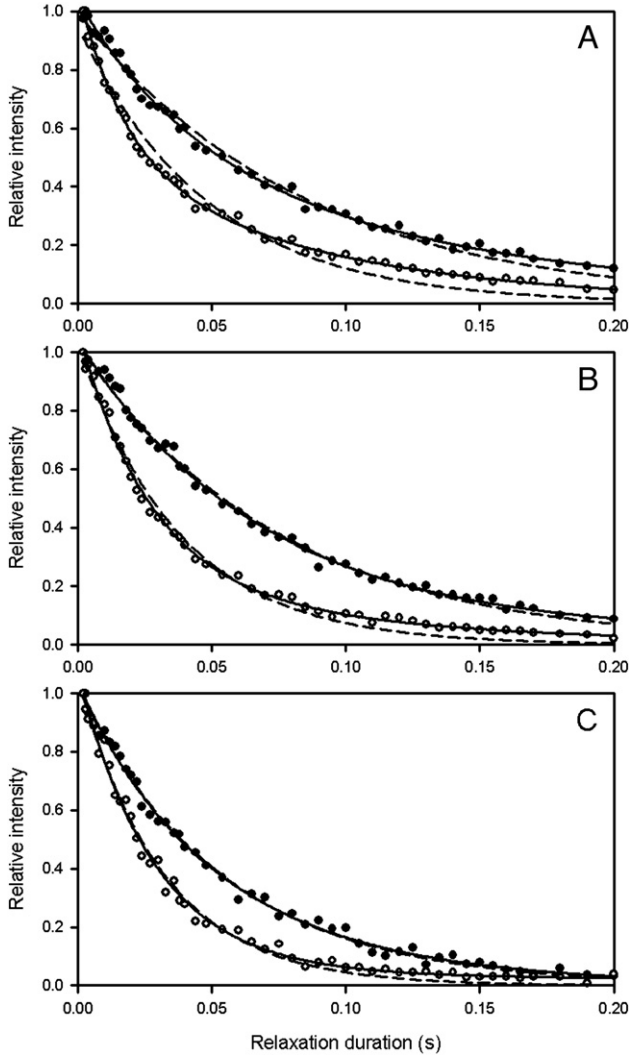

Fig. 4. Single-spin-state ^{15}N relaxation R_α (●) and R_β (○) decay curves of ElonBC-SB obtained using the TRACT sequence at temperatures 283 K (A), 288 K (B) and 293 K (C). As in Fig. 3, dashed and solid lines represent the results of nonlinear regression of single and dual two-parameter single exponential decays, respectively.

program *tmest* within the Modelfree software package (A. G. Palmer, Columbia University).

Effective rotational correlation times of ElonBC-SB derived from both translational diffusion coefficients and collective ^{15}N relaxation rates over the temperature range studied are shown in Fig. 5. While values of rotational correlation times of ElonBC-SB derived from translational diffusion coefficients and collective single-spin-state ^{15}N relaxation rates differ, both can be described by the Vogel–Fulcher–Tamman (VFT) equation (Fig. 5B), $\tau_c=\tau_0\exp(AT_0/(T-T_0))$, where τ_0, A and T_0 are fitting parameters, reflecting that the diffusive behavior of ElonBC-SB is consistent with the Debye–Stokes–Einstein model across the temperature range. In contrast, rotational correlation times at lower temperatures, derived from collective R_2/R_1 ratios measured from conventional relaxation-weighted HSQC spectra, clearly deviated from the VFT equation, suggesting they are not an adequate reflection of the true τ_c values.

Rotational correlation times from collective backbone single-spin-state ^{15}N relaxation rates, R_α and R_β, have been shown previously to give reasonable τ_c values [6]. However, in the case of a protein domain containing flexible loops and termini, collective backbone ^{15}N relaxation rates gave rotational correlation time significantly lower than the value from residue-specific relaxation analyses [5]. It was also observed that ^{15}N relaxation R_1 and R_2 rates obtained from the first-increment FIDs of relaxation-weighted HSQC spectra were significantly different from the averaged R_1 and R_1 values calculated from values measured for individual residues [5]. For collective ^{15}N relaxation rates the presence of flexible termini and/or loops becomes much more significant, particularly for R_2, as the collective relaxation rates are dominated by residues from flexible termini and/or loops. In this study, τ_c estimated from the faster component of collective R_2 values (resulting from the fit of a dual two-parameter exponential decay approximation using average first-increment FIDs of ^{15}N R_2 weighted ^{15}N-HSQC spectra acquired with a conventional pulse sequence) was reasonable at higher (310 and 318 K) but not at lower temperatures (Fig. 5). This indicates that even the faster component resulting from a dual exponential decay approximation fails to produce a sufficiently reliable R_2 value for backbone amides with minimal influence from internal motion. In contrast, we found that single-spin-state ^{15}N relaxation rates, R_α and R_β, as measured using the TRACT sequences, gave reasonable, lower limit, estimations of τ_c provided fits to a dual exponential decay rather than a single exponential decay were performed. Thus, when estimating protein effective rotational times in solution using collective ^{15}N relaxation rates, it appears that the conventional sequences are more susceptible to the presence of flexible termini and/or loop regions than the newly introduced single-spin-state TRACT sequences.

In contrast to effective rotational correlation times derived from collective backbone ^{15}N relaxation parameters, effective rotational correlation times calculated from translational diffusion coefficients using Eq. (6) agree well with τ_c values derived from residue-specific relaxation analysis and those calculated from the structure of a highly

Table 2
Collective backbone ^{15}N relaxation rates and rotational correlations of ElonBC-SB

T (K)	R_1 (s^{-1})	R_2^a (s^{-1})	R_{2f}, R_{2s}^b (s^{-1})	R_{2f}/R_1^c	τ_c^d (ns)	R_α (s^{-1})	$R_{\alpha f}$, $R_{\alpha s}$ (s^{-1})	R_β (s^{-1})	$R_{\beta f}$, $R_{\beta s}$ (s^{-1})	τ_c^e (ns)
283	1.31±0.04	4.9±0.4	17.4±3.7 2.9±0.40	12.3±2.9	10.9±1.5	10.3±0.2	17.8±4.2 5.0± 2.6	16.2±0.7	69.6±5.2 10.5±0.4	25.1
288	1.24±0.05	5.0±0.5	19.6± 3.5 2.6±0.3	15.8±2.9	12.4±1.3	12.1±0.2	23.0±6.4 7.4± 2.2	20.7±0.8	56.4±4.5 11.6±0.7	16.0
293	1.26±0.06	5.8±0.4	15.0±0.9 2.5±0.2	11.9±0.9	10.7±0.5	12.3±0.2	15.4±2.2 1.4±6.4	22.9±0.8	47.7±3.8 10.7±1.1	15.4
298	1.18±0.04	6.8±0.6	15.9±1.9 1.9±0.4	13.5±1.7	11.4±0.8	13.4±0.2	–	26.3±0.7	38.1±3.4 10.1±2.6	11.7
310	1.14±0.05	8.7±0.6	15.1±2.3 2.1±1.0	13.2±2.1	11.3±1.0	14.8±0.6	–	31.5±1.2	–	7.6
318	1.39±0.13	9.9±0.3	–	7.1±0.7	7.9±0.5	18.1±0.6	–	30.8±0.9	–	5.4

[a] Single-component two-parameter fit (relaxation rates and standard errors of nonlinear regression are shown).
[b] Two-component dual two-parameter fit.
[c] Collective ^{15}N R_{2f}/R_1 ratios (calculated using R_{2f}, the faster component from a dual two-parameter exponential fit).
[d] Effective rotational correlation times calculated from the collective ^{15}N R_{2f}/R_1 ratios.
[e] Effective rotational correlation times calculated from the difference of collective single-spin-state ^{15}N relaxation rates of backbone amides, $R_\beta - R_\alpha$ [6].

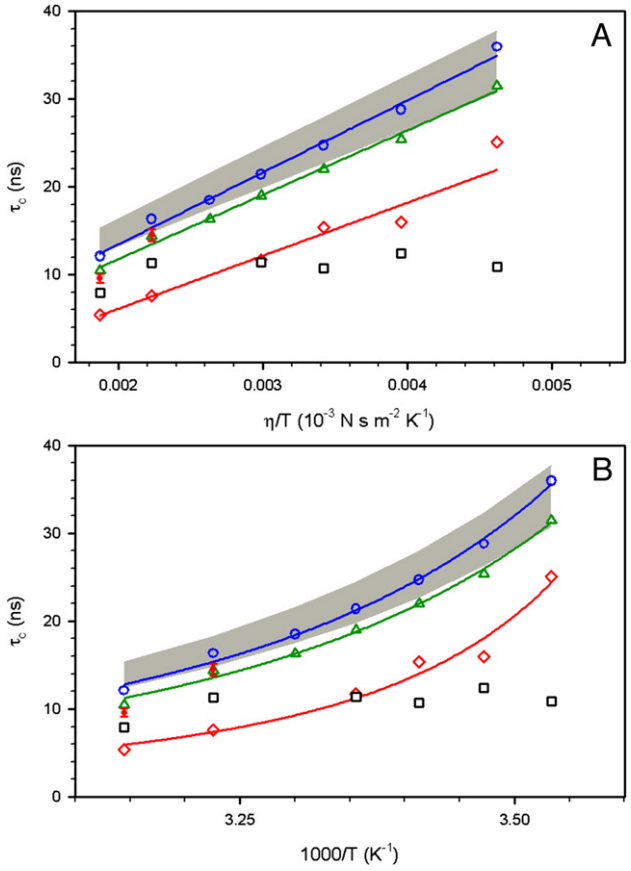

Fig. 5. Effective rotational correlation times versus η/T (A) and $1000/T$ (B) derived from (□) collective ^{15}N relaxation parameters ^{15}N R_2/R_1 ratio of first-increment FIDs of relaxation-weighted ^{15}N-HSQC spectra; (◊) single-spin-state TRACT sequences, (○) translational diffusion coefficients and (Δ) calculated from hydrodynamic radii (using values given in Table 2 and the viscosities of water as an approximation). Lines in A represent linear regression fits to the data and pass through the origin as described by the Stokes–Einstein equation, whereas lines in B represent fitting to the Vogel–Fulcher–Tamman (VFT) equation. The shaded bands represent rotational correlation times of ElonBC-SB as calculated from the crystal structure of elonginBC+SOCS-2$^{160-198}$ with atomic element radii (AER) of 3.1 and 5.0 Å, respectively. Rotational correlation times, τ_c, at 310 and 318 K determined using averaged R_2/R_1 ratios of residues from well ordered and structured regions of the complex are indicated as vertical bars with their lengths corresponding to the error ranges (⧳).

similar protein complex solved by X-ray crystallography. We note that τ_c values derived from translational diffusion coefficients appear to be slightly longer than those derived from the residue-specific ^{15}N relaxation analysis (Fig. 5). The difference between effective rotational correlation times estimated from backbone ^{15}N relaxation time and translational diffusion coefficients (Fig. 5) may, to some extent, reflect the internal motion possessed by those backbone amides used for the determination of τ_c from their relaxation parameters, as any internal motion will lead to an underestimated τ_c [24]. The apparent overestimated τ_c values from translational diffusion coefficients, as can be seen from Eq. (6), could also be a consequence of: (1) experimentally measured translational diffusion coefficients are somewhat under estimated (as observed previously that experimentally measured translational diffusion coefficients are systematically smaller than theoretically calculated values [23]) and/or (2) the hydrodynamic radius of the reference molecule, R_h^{REF}, is over estimated (i.e. the hydrodynamic radius of dioxane is in fact less than 2.12 Å as reported previously [12].). Nevertheless, translational diffusion coefficients, which can be readily measured by PFG-NMR under identical solution conditions to those used for other studies, such as molecular structural and interaction studies, and without the need for isotopically labelled materials, can be used to for rapid estimates of protein effective rotational correlation times. Finally, these values derived from translational diffusion coefficients may also be considered as an experimentally determined upper limit of the effective rotational correlation time (Fig. 5). Together with values determined from collective relaxation measurements the range of the effective rotational correlation times of a protein in a given solution condition can be defined experimentally.

It is worth noting that dioxane, even though it is a small molecule, appears to function well as an internal standard for a relatively large complex like ElonBC-SB (~30 kDa). Small molecules other than dioxane have been used previously as internal references in translational diffusion measurements in order to facilitate comparisons between samples with different solution conditions [25,26]. For small molecules other than dioxane to be used as internal references for the estimation of effective rotational correlation times, indicative values of R_h are needed. We have carried out measurements of several other small molecules, namely DMSO, acetone, and acetonitrile, in the presence of dioxane under similar solution conditions to those used for ElonBC-SB and the results are summarized in Table 3. Representative diffusion weighted spectra and diffusion induced peak intensities decay curves are shown in Supplementary data (Fig. S3). Over the temperature range 283–318 K, all three molecules behave as well as dioxane and the measurements resulted in indicative hydrodynamic radii of 1.97, 1.77, and 1.40 Å for DMSO, acetone, and acetonitrile, respectively. As DMSO, acetone, and acetonitrile give rise to resonances at chemical shifts different from dioxane (Fig. S3A, Supplementary data), they may be of use when accurate measurements of diffusion coefficients of dioxane become problematic due to spectral overlap. Finally, translational diffusion coefficients of EDTA in the absence of ElonBC-SB (Table 3) agree very well with those obtained in the presence of ElonBC-SB (Table 1) with an indicative hydrodynamic radius of approximately 4.50 Å.

Table 3
Translational diffusion coefficients and hydrodynamic radii of alternative small molecules

	Dioxane (88 Da)		DMSO (78 Da)		Acetone (58 Da)		Acetonitrile (48 Da)		EDTA (292 Da)	
T (K)	D^a (10^{-9} m^2 s^{-1})	R_h (Å)	D^a (10^{-9} m^2 s^{-1})	R_h^b (Å)	D^a (10^{-9} m^2 s^{-1})	R_h^b (Å)	D^a (10^{-9} m^2 s^{-1})	R_h^b (Å)	D^a (10^{-9} m^2 s^{-1})	R_h^b (Å)
283	0.67±0.01	2.12	0.72±0.01	1.97	0.80±0.01	1.78	1.03±0.01	1.38	0.31±0.01	4.58
288	0.80±0.01	2.12	0.85±0.01	2.00	0.95±0.01	1.79	1.21±0.01	1.40	0.37±0.01	4.58
293	0.92±0.01	2.12	0.98±0.02	1.99	1.09±0.02	1.79	1.39±0.03	1.40	0.42±0.01	4.64
298	1.06±0.01	2.12	1.14±0.01	1.97	1.27±0.01	1.77	1.61±0.01	1.40	0.50±0.01	4.49
303	1.21±0.01	2.12	1.31±0.01	1.96	1.46±0.01	1.76	1.85±0.01	1.39	0.58±0.01	4.42
310	1.43±0.01	2.12	1.54±0.01	1.97	1.72±0.01	1.76	2.17±0.01	1.40	0.68±0.01	4.46
318	1.71±0.01	2.12	1.83±0.01	1.98	2.05±0.01	1.77	2.56±0.01	1.42	0.81±0.01	4.48

[a] Translational diffusion coefficients shown are average value±standard deviation calculated from eight measurements with diffusion encoding gradients applied either in the x or y direction.

[b] R_h values for DMSO, acetone, acetonitrile, and EDTA calculated using Eq. (5) with an R_h of 2.12 Å for dioxane. Mean R_h values for DMSO, acetone, acetonitrile, and EDTA are 1.97±0.01, 1.77±0.01, 1.40±0.01, and 4.52±0.08 Å, respectively.

4. Conclusions

We have shown that, provided the protein diffusive behavior is coherent with the Debye–Stokes–Einstein model, translational diffusion coefficients provide a means for quick estimates of rotational correlation times with reasonable accuracy, which may be otherwise difficult to determine from alternative rapid methods, such as collective backbone ^{15}N relaxation rates. Translational diffusion coefficients provide rapid estimates of protein rotational correlation times with the advantages that the protein of interest does not need to be isotopically labelled and the resulting τ_c is not susceptible to internal motion of the protein. This approach to determining effective rotational correlation times may be particularly useful in studies of biomolecular structure and interactions in situations where i) isotopically labelled material is not available, ii) collective backbone ^{15}N relaxation rates are difficult to interpret because of the presence of flexible termini or loops, such as in intrinsically unstructured proteins, or iii) a full relaxation analysis is practically difficult because of limited sensitivity owing to low protein concentration, high molecular mass or low temperatures).

Acknowledgements

This work was supported in part by the Australian National Health and Medical Research Council (NHMRC) (Program grant 461219). We thank Arthur Palmer (Columbia University) for valuable comments and Mark Hinds for thoughtful discussions.

Appendix A. Supplementary data

Supplementary data associated with this article can be found, in the online version, at doi:10.1016/j.bpc.2008.06.002.

References

[1] N. Tjandra, S.E. Feller, R.W. Pastor, A. Bax, Rotational diffusion anisotropy of human ubiquitin from ^{15}N NMR relaxation, J. Am. Chem. Soc. 117 (1995) 12562–12566.
[2] L.E. Kay, D.A. Torchia, A. Bax, Backbone dynamics of proteins as studied by ^{15}N inverse detected heteronuclear NMR-spectroscopy — application to staphylococcal nuclease, Biochemistry 28 (1989) 8972–8979.
[3] S. Yao, M.G. Hinds, R.S. Norton, Improved estimation of protein rotational correlation times from ^{15}N relaxation measurements, J. Magn. Reson. 131 (1998) 347–350.
[4] D.S. Korchuganov, I.E. Gagnidze, E.N. Tkach, A.A. Schulga, M.P. Kirpichnikov, A.S. Arseniev, Determination of protein rotational correlation time from NMR relaxation data at various solvent viscosities, J. Biomol. NMR 30 (2004) 431–442.
[5] Z. Kuang, S. Yao, D.W. Keizer, C.C. Wang, L.A. Bach, B.E. Forbes, J.C. Wallace, R.S. Norton, Structure, dynamics and heparin binding of the C-terminal domain of insulin-like growth factor-binding protein-2 (IGFBP-2), J. Mol. Biol. 364 (2006) 690–704.
[6] D. Lee, C. Hilty, G. Wider, K. Wüthrich, Effective rotational correlation times of proteins from NMR relaxation interference, J. Magn. Reson. 178 (2006) 72–76.
[7] W.S. Price, F. Tsuchiya, Y. Arata, Lysozyme aggregation and solution properties studied using PGSE NMR diffusion measurements, J. Am. Chem. Soc. 121 (1999) 11503–11512.
[8] S. Yao, G.J. Howlett, R.S. Norton, Peptide self-association in aqueous trifluoroethanol monitored by pulsed field gradient NMR diffusion measurements, J. Biomol. NMR 16 (2000) 109–119.
[9] T. Brand, E.J. Cabrita, G.A. Morris, R. Gunther, H.J. Hofmann, S. Berger, Residue-specific NH exchange rates studied by NMR diffusion experiments, J. Magn. Reson. 187 (2007) 97–104.
[10] A. Dehner, H. Kessler, Diffusion NMR spectroscopy: folding and aggregation of domains in p53, Chembiochem. 6 (2005) 1550–1565.
[11] L.H. Lucas, C.K. Larive, Measuring ligand–protein binding using NMR diffusion experiments, Concepts Magn. Reson. Part A 20A (2004) 24–41.
[12] D.K. Wilkins, S.B. Grimshaw, V. Receveur, C.M. Dobson, J.A. Jones, L.J. Smith, Hydrodynamic radii of native and denatured proteins measured by pulse field gradient NMR techniques, Biochemistry 38 (1999) 16424–16431.
[13] V.Y. Orekhov, D.M. Korzhnev, K.V. Pervushin, E. Hoffmann, A.S. Arseniev, Sampling of protein dynamics in nanosecond time scale by ^{15}N NMR relaxation and self-diffusion measurements, J. Biomol. Struct. Dyn. 17 (1999) 157–174.
[14] M. Zeeb, M.H. Jacob, T. Schindler, J. Balbach, ^{15}N relaxation study of the cold shock protein CspB at various solvent viscosities, J. Biomol. NMR 27 (2003) 221–234.
[15] P.T. Callaghan, M.A. Legros, D.N. Pinder, The measurement of diffusion using deuterium pulsed field gradient nuclear magnetic resonance, J. Chem. Phys. 79 (1983) 6372–6381.
[16] S.J. Gibbs, C.S. Johnson, A PFG NMR experiment for accurate diffusion and flow studies in the presence of eddy currents, J. Magn. Reson. 93 (1991) 395–402.
[17] M. Piotto, V. Saudek, V. Sklenar, Gradient-tailored excitation for single-quantum NMR spectroscopy of aqueous solutions, J. Biomol. NMR 2 (1992) 661–665.
[18] J.A. Jones, D.K. Wilkins, L.J. Smith, C.M. Dobson, Characterisation of protein unfolding by NMR diffusion measurements, J. Biomol. NMR 10 (1997) 199–203.
[19] N.A. Farrow, R. Muhandiram, A.U. Singer, S.M. Pascal, C.M. Kay, G. Gish, S.E. Shoelson, T. Pawson, J.D. Formankay, L.E. Kay, Backbone dynamics of a free and a phosphopeptide-complexed Src homology-2 domain studied by ^{15}N NMR relaxation, Biochemistry 33 (1994) 5984–6003.
[20] A.N. Bullock, J.E. Debreczeni, A.M. Edwards, M. Sundstrom, S. Knapp, Crystal structure of the SOCS2-elongin C-elongin B complex defines a prototypical SOCS box ubiquitin ligase, Proc. Natl. Acad. Sci. U. S. A. 103 (2006) 7637–7642.
[21] J. Garcia de la Torre, M.L. Huertas, B. Carrasco, HYDRONMR: prediction of NMR relaxation of globular proteins from atomic-level structures and hydrodynamic calculations, J. Magn. Reson. 147 (2000) 138–146.
[22] R.C. Weast, CRC Handbook of Chemistry and Physics, Boca Raton, FL, 1984.
[23] V.V. Krishnan, Determination of oligomeric state of proteins in solution from pulsed-field-gradient self-diffusion coefficient measurements. A comparison of experimental, theoretical, and hard-sphere approximated values, J. Magn. Reson. 124 (1997) 468–473.
[24] D.M. Korzhnev, V.Y. Orekhov, A.S. Arseniev, Determination of protein rotational correlation time from NMR relaxation data at various solvent viscosities, J. Magn. Reson. 127 (1997) 184–191.
[25] E.J. Cabrita, S. Berger, DOSY studies of hydrogen bond association: tetramethylsilane as a reference compound for diffusion studies, Magn. Reson. Chem. 39 (2001) S142–S148.
[26] C.A. Crutchfield, D.J. Harris, Molecular mass estimation by PFG NMR spectroscopy, J. Magn. Reson. 185 (2007) 179–182.